

Stereographic coordinates for simpler far-field radiation analysis

Vassili Savinov
Independent Researcher
Southampton
United Kingdom
vsavinov@protonmail.com

A coordinate system is proposed for the purposes of analysis of far-field radiation from a localized source at the origin. The proposed coordinates exhibit no singularities over the far-field hemi-sphere, making them a good choice for automated radiation pattern analysis. Finally, it is shown that Ludwig polarization basis, commonly used to represent polarization of the far-field radiation, arises naturally, as a coordinate basis, when one uses stereographic coordinates.

I. INTRODUCTION

Evaluation of far-field radiation is a common task in antenna as well as optical engineering. Distribution of radiation over the surface of an imaginary sphere or hemi-sphere, with extremely large radius, centered on the localized source of electromagnetic waves, is scrutinized in terms of intensity, directivity, polarization state purity, coherence as well as other key metrics [1].

To describe the distribution of the electromagnetic field on the far-field sphere, it is natural to use spherical coordinate system as well as spherical basis, for vector decomposition [2]. Given extraordinarily detailed theory of spherical coordinates [3], [4], developed by generations of scientists and engineers, working with them presents no serious difficulties for a skilled practitioner. Getting computer algorithm to handle outputs in spherical coordinates, however, can be a time-consuming exercise. The main difficulty stems from handling the edge-cases presented by coordinate singularities at south and north poles of the sphere, as well as the cyclic nature of the azimuthal angle. Consider, for example, developing an algorithm to compute and average value of electric field over a small, but finite solid angle that could or could not include one of the poles. One can certainly develop a robust and stable algorithm to handle such cases, but there will be a price to pay in terms of human time spent developing and maintaining the code. A better way to approach such problems is to develop a suitable mathematical framework that removes edge-cases by design.

Here we consider a mathematical solution to a slightly simpler, but nevertheless common problem - analysis of far-field radiation on the surface of a *hemi*-sphere. The key difference is that unlike the full sphere, the surface of a hemi-sphere can be described using Cartesian-like coordinates, i.e.

the surface of a hemi-sphere can be mapped smoothly onto two-dimensional plane [5]. We develop key scalar and vector properties of one possible choice for such coordinates, the stereographic coordinates. In the process, we demonstrate that Ludwig basis [6], a popular choice for decomposing vector fields tangent to a sphere is essentially the (normalized) coordinate basis for stereographic coordinates. Finally, we present visualization and basic analysis of far-field radiation from an illuminated aperture, in stereographic coordinates.

II. STEREOGRAPHIC PROJECTION AND STEREOGRAPHIC COORDINATES

The roots of stereographic projection go back to the ancient Greece, and in particular to work of Hipparchos. Whilst initial application of stereographic projection was limited to astronomy, cartography and navigation, its utility has since been recognized in crystallography (e.g. Wulff net) and geology. A detailed historical account of stereographic projection development and application has been compiled by Howarth [7]. Key mathematical properties of the projection have been summarized by Rosenfeld and Sergeeva [8]. Despite the wide-spread use of stereographic projection in geo-sciences [9], [10], as well as engineering and material science [8], [7], [11], [12], [13], it remains relatively unknown in the field of applied electromagnetism. In this section we provide two definitions of the stereographic projection: geometric and algebraic.

The geometric definition of stereographic projection involves placing a sphere, the surface of which is to be projected, with north- and south-poles at z -axis, so that equator would lie in the $z = 0$ plane, then drawing straight lines emanating from south-pole. The point at which the straight line intersects the sphere is then mapped onto point at which the same line intersects the $z = 0$ plane. The method is illustrated in Fig. 1a. All of the sphere, except for the south-pole, can be mapped onto a flat plane in this manner, however it is common to only map one hemi-sphere, e.g. the north hemi-sphere, since mapped structures become progressively more distorted as one comes closer to the south pole.

The algebraic definition of stereographic projection of an arbitrary point (r, θ, ϕ) in 3-dimensional space, in spheri-

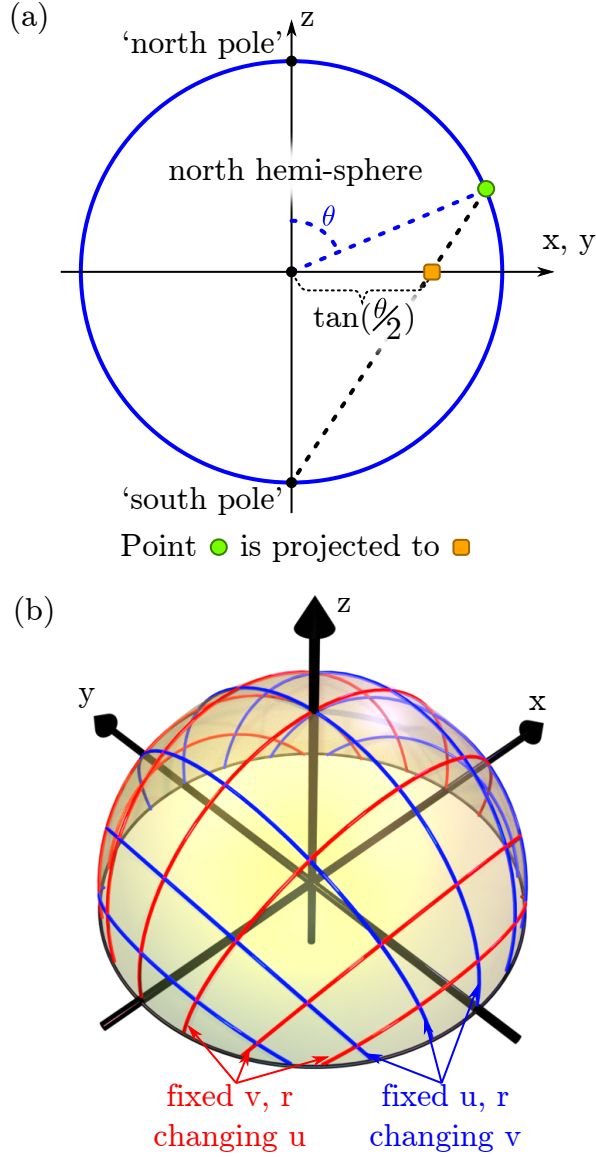


Figure 1. Illustration of stereographic projection and stereographic coordinates. (a) Geometric construction of the stereographic projection. A point on a sphere is mapped onto a point on a 2d plane. Here, for simplicity, we show a circle instead of the sphere and a line instead of the plane. A chosen point on the circle (green circle), which corresponds to angle θ , is projected onto the horizontal axis by plotting a straight line from the south pole of the circle to the chosen point. The point at which the straight line intersects the horizontal axis corresponds to the position of the projected point (orange square). Formally, all points on the surface of a sphere, parameterized by (θ, ϕ) , are projected onto points on a plane with Cartesian coordinates $(\tan \frac{\theta}{2} \cos \phi, \tan \frac{\theta}{2} \sin \phi)$. (b) Grid generated by stereographic coordinates on a surface of a hemi-sphere. One of the stereographic coordinates is the radius r , which remains constant on the hemi-sphere. The other two coordinates are u and v . Red curves are generated by fixing v (and r), and varying u within the limits set by $u^2 + v^2 = 1$, blue curves, correspondingly, are generated by fixing u and varying v .

cal coordinates, to point (ξ, η) in 2-dimensional space, in Cartesian coordinates, is:

$$\xi = \cos \phi \cdot \tan \frac{\theta}{2} \quad (1)$$

$$\eta = \sin \phi \cdot \tan \frac{\theta}{2} \quad (2)$$

The projection remains well-defined for all points with $0 \leq \theta < \pi$. Note that $\xi^2 + \eta^2 = \tan^2 \theta/2$, thus all points, on the sphere, with $\theta \leq \pi/2$ are mapped inside the unit-radius circle on the $\xi\eta$ -plane. Thus stereographic projection, as defined above, projects all points in the $z \geq 0$ half-space into a circle with unit radius in the $\xi\eta$ -plane.

A. Stereographic coordinates

Based on inverse stereographic projection, i.e. mapping unit-radius circle to a surface of a hemi-sphere, one can define *stereographic coordinates* for $z \geq 0$ half-space. The stereographic coordinates of an arbitrary point P in $z \geq 0$ half-space are u, v and r . The latter (r) is the distance from the origin to P , equivalently it is the radius of the hemi-sphere that contains the point on its surface. Coordinates u and v are the coordinates that point P would have if it were mapped onto a unit-circle with stereographic projection.

Figure 1b shows the curves generated by fixing r as well as either u or v , and varying the other. Crucially, the curves of varying u , i.e. the red curves in Fig. 1b, do not intersect, and the same applies to curves of varying v . This is a visual illustration of an important property of the stereographic coordinates - lack of the coordinate singularities. Stereographic coordinates allow one to describe any point on a hemi-sphere in the same way as one would describe any point inside a unit circle - with two Cartesian coordinates. Coordinates u and v can vary within the range $-1 \dots 1$, and any combination of these coordinates will be valid (only the points with $u^2 + v^2 \leq 1$ will be on the northern hemi-sphere). Furthermore, if two points on a hemi-sphere are close to each other, their u and v coordinates will always be close as well. Contrast this with, spherical coordinates, where $\phi = 0$ and $\phi = 2\pi$ correspond to the same location on a surface of the sphere, despite the large difference in the value of the coordinate. This well-behavedness lends itself readily for use in numerical analysis of, for example, far-field radiation patterns, which will be discussed in Sec. IV.

The mapping between spherical coordinates and stereographic coordinates, for $\theta \leq \pi/2$, is given by (r is common to both spherical and stereographic coordinates):

$$u = \cos \phi \cdot \tan \frac{\theta}{2} \quad (3)$$

$$v = \sin \phi \cdot \tan \frac{\theta}{2} \quad (4)$$

$$\theta = 2 \arctan \left(\sqrt{u^2 + v^2} \right) \quad (5)$$

$$\phi = \arctan \left(\frac{v}{u} \right) \quad (6)$$

Mapping between Cartesian and stereographic coordinates is:

$$u = \frac{x}{r+z} \quad (7)$$

$$v = \frac{y}{r+z} \quad (8)$$

$$r = \sqrt{x^2 + y^2 + z^2} \quad (9)$$

III. STEREOGRAPHIC BASIS AND LUDWIG BASIS

One of the basic results in antenna theory is that far-field radiation from a localized electromagnetic source is of transverse polarization [2], i.e. tangent to the far-field sphere. Consequently, far-field radiation can be expressed in spherical basis vectors $\hat{\theta}$ (points from north to south pole, along the meridians) and $\hat{\phi}$ (points west to east along parallels). However, use of spherical basis becomes challenging at the poles of the hemi-sphere, where coordinate singularity renders the spherical basis ill-defined. Ludwig polarization basis [6], [2] solves this problem by introducing basis vectors:

$$\hat{\mathbf{i}}_{ref} = \sin \phi \hat{\theta} + \cos \phi \hat{\phi} \quad (10)$$

$$\hat{\mathbf{i}}_{cross} = \cos \phi \hat{\theta} - \sin \phi \hat{\phi} \quad (11)$$

Which are transverse, i.e. tangent to far-field sphere, orthonormal, and well-behaved at poles. Here we will show that stereographic coordinates naturally give rise to Ludwig basis.

Consider the coordinate basis of stereographic coordinates on the surface of far-field hemi-sphere. The radial vector $\hat{\mathbf{r}}$ is the same as in spherical coordinates, and will therefore be skipped in the following discussion. The coordinate basis vectors for u and v , i.e. tangents to the curves of varying u and v (see Fig. 1b), are: $\mathbf{e}_u = \frac{d}{du}$ and $\mathbf{e}_v = \frac{d}{dv}$ correspondingly. Here we follow conventions of differential geometry in defining vectors as tangents to curves [14]. This is the coordinate basis for the uv -coordinates on the far-field hemi-sphere. Using Eq. (3, 4), the relationship to the corresponding spherical coordinate basis is then given by:

$$\begin{aligned} \mathbf{e}_\theta &= \frac{d}{d\theta} = \frac{\partial u}{\partial \theta} \mathbf{e}_u + \frac{\partial v}{\partial \theta} \mathbf{e}_v = \frac{\cos \phi}{2 \cos^2 \frac{\theta}{2}} \mathbf{e}_u + \frac{\sin \phi}{2 \cos^2 \frac{\theta}{2}} \mathbf{e}_v \\ &= \frac{1+u^2+v^2}{2\sqrt{u^2+v^2}} (u\mathbf{e}_u + v\mathbf{e}_v) \\ \mathbf{e}_\phi &= \frac{d}{d\phi} = \frac{\partial u}{\partial \phi} \mathbf{e}_u + \frac{\partial v}{\partial \phi} \mathbf{e}_v \\ &= -\tan \frac{\theta}{2} \sin \phi \mathbf{e}_u + \tan \frac{\theta}{2} \cos \phi \mathbf{e}_v \\ &= -v\mathbf{e}_u + u\mathbf{e}_v \end{aligned}$$

Converting to more familiar normalized basis for spherical coordinates: $\hat{\theta} = \mathbf{e}_\theta / r$, $\hat{\phi} = \mathbf{e}_\phi / r \sin \theta$:

$$\hat{\theta} = \frac{1+u^2+v^2}{2r\sqrt{u^2+v^2}} (u\mathbf{e}_u + v\mathbf{e}_v)$$

$$\hat{\phi} = \frac{1+u^2+v^2}{2r\sqrt{u^2+v^2}} (-v\mathbf{e}_u + u\mathbf{e}_v)$$

Similar approach, with Eq. (5, 6), can be used to invert the relations:

$$\mathbf{e}_u = \frac{2r}{(1+u^2+v^2)\sqrt{u^2+v^2}} (u\hat{\theta} - v\hat{\phi})$$

$$\mathbf{e}_v = \frac{2r}{(1+u^2+v^2)\sqrt{u^2+v^2}} (v\hat{\theta} + u\hat{\phi})$$

Clearly, $\mathbf{e}_u \cdot \mathbf{e}_v = 0$ and $\mathbf{e}_u \cdot \mathbf{e}_u = \mathbf{e}_v \cdot \mathbf{e}_v = 4r^2 / (1+u^2+v^2)^2$. One can then define normalized stereographic basis as $\hat{\mathbf{u}} = \mathbf{e}_u (1+u^2+v^2) / 2r$, $\hat{\mathbf{v}} = \mathbf{e}_v (1+u^2+v^2) / 2r$, then:

$$\hat{\theta} = \frac{1}{\sqrt{u^2+v^2}} (u\hat{\mathbf{u}} + v\hat{\mathbf{v}}) \quad (12)$$

$$\hat{\phi} = \frac{1}{\sqrt{u^2+v^2}} (-v\hat{\mathbf{u}} + u\hat{\mathbf{v}}) \quad (13)$$

Finally, substituting Eq. (12, 13) into Eq. (10, 11) one finds:

$$\hat{\mathbf{i}}_{ref} = \hat{\mathbf{v}} = \frac{1+u^2+v^2}{2r} \mathbf{e}_v \quad (14)$$

$$\hat{\mathbf{i}}_{cross} = \hat{\mathbf{u}} = \frac{1+u^2+v^2}{2r} \mathbf{e}_u \quad (15)$$

Ludwig basis is the normalized coordinate basis of the stereographic coordinates.

One of the great utilities of coordinate basis is in providing a simple form for common vector calculus operations. For example, for any suitably smooth scalar field $f = f(u, v, r)$, its gradient is given by:

$$\begin{aligned} \nabla f &= \frac{\alpha}{2r} \frac{\partial f}{\partial u} \hat{\mathbf{u}} + \frac{\alpha}{2r} \frac{\partial f}{\partial v} \hat{\mathbf{v}} + \frac{\partial f}{\partial r} \hat{\mathbf{r}} \\ &= \frac{\alpha}{2r} \frac{\partial f}{\partial u} \hat{\mathbf{i}}_{cross} + \frac{\alpha}{2r} \frac{\partial f}{\partial v} \hat{\mathbf{i}}_{ref} + \frac{\partial f}{\partial r} \hat{\mathbf{r}} \end{aligned}$$

where $\alpha = 1+u^2+v^2$ (to improve readability). See Supplementary Materials (Sec. VI) for further details, including expressions for divergence and curl in stereographic coordinates. Simplicity in extracting numerically well-behaved gradient, curl and divergence can be of great utility in developing algorithms for identifying and scrutinizing key metrics of far-field radiation from an antenna.

IV. APPLICATION OF STEREOGRAPHIC COORDINATES: VISUALIZATION OF FAR-FIELD RADIATION FROM UNIFORMLY ILLUMINATED APERTURE

As an application of stereographic coordinates, here we visualize the far-field radiation from a square aperture that lies in the XY-plane, at the origin. The size of the aperture is a , its sides are aligned to lie parallel to x and y axis. The (time-harmonic) electric field at the aperture follows:

$$\mathbf{E} = \hat{\mathbf{x}} \cdot E_0 \cdot \exp(-i(\zeta_x x + \zeta_y y)) \cdot \exp(i\omega t), \quad -\frac{a}{2} \leq x, y \leq \frac{a}{2}$$

and is zero at all other points on the $z = 0$ plane. The phase gradient was set to $\zeta_x = 0.3k_0$ and $\zeta_y = 0.6k_0$, where $k_0 = 4\pi/a$. The angular frequency is $\omega = 4\pi c/a$, where c is the speed of light, t is time, and E_0 is the amplitude

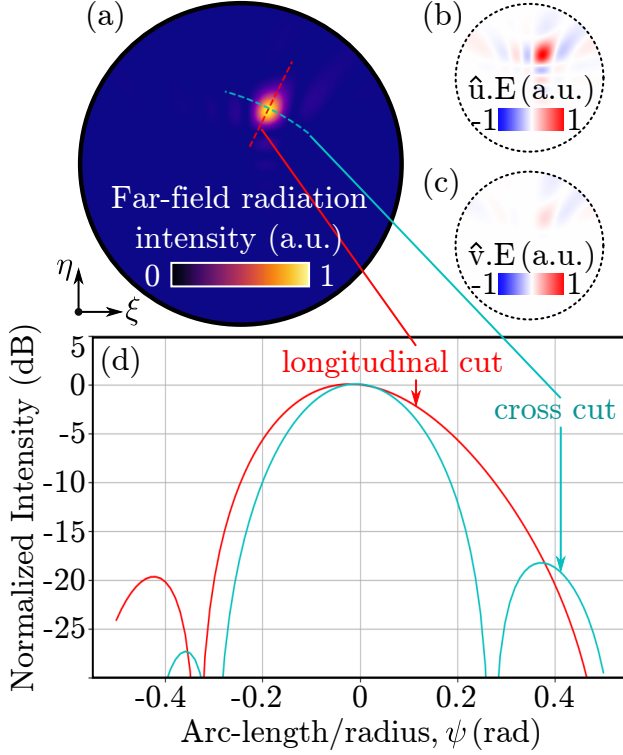


Figure 2. **Visualization of far-field radiation from square aperture source.** The source electric field at the $z = 0$ plane is $\mathbf{E} = \hat{\mathbf{x}} \cdot E_0 \cdot \exp(-i(\zeta_x x + \zeta_y y)) \cdot \exp(i\omega t)$ inside the aperture and zero everywhere else. The phase gradient is $\zeta_x = 0.3k_0$ and $\zeta_y = 0.6k_0$, where $k_0 = \omega/c$ is the wavenumber of the radiation (and c is the speed of light). The wavelength of radiation is $\lambda_0 = a/2$, where a is the size of the square aperture. (a) Stereographic projection of the intensity of the radiation, shown as colormap, emitted into the north hemisphere. (b), (c) Show the colormaps of the components of the far-field electric field along \hat{u} and \hat{v} respectively. (d) Shows the cuts through the intensity peak as a function of normalized arc-length of the cut curve. Since the arc-length is normalized with respect to the radius of the hemisphere, its units are radians. The cuts are also depicted in (a).

of the electric field. The ambient environment is vacuum. The relevant wavelength of the radiation at frequency ω is $\lambda_0 = a/2$.

The full expression for the far-field radiation from the source described above, in stereographic coordinates, is given in the Appendix (see App. VIII). Since the expression for the radiation pattern, in spherical coordinates, is well-known [2], and its conversion to stereographic coordinates is a straightforward algebraic exercise, here we focus only on the visualization of the radiation pattern. Figure 2a, shows the intensity of the far-field radiation over the $z \geq 0$ hemisphere, projected into a circle via the stereographic projection. To avoid confusion, we define ξ, η to be the Cartesian coordinates on the plane used for visualization, i.e. the plane of Fig. 2a. The stereographic projection of a point at (u, v, r) , in 3d stereographic coordinates, onto the visualization plane can then be expressed as $\xi = u$ and $\eta = v$. Figures 2b,c show the $\hat{u} = \hat{i}_{cross}$ and $\hat{v} = \hat{i}_{ref}$ components of the electric field, respectively. The nature

of stereographic projection means that \hat{u} -polarized fields in stereographic coordinates will be pointing horizontally, i.e. along $\hat{\xi}$, on the $\xi\eta$ -plane, after projection. Correspondingly, the \hat{v} -polarized fields will be projected into the vertically-pointed fields on $\xi\eta$ -plane.

Figure 2d shows the meridional and cross cuts through the peak of the radiation intensity. The same cuts are also indicated in Fig. 2a. Both meridional and cross cuts are along the so-called great circles [14], i.e. the curves that correspond to ‘straight’ lines on a spherical surface (geodesics). An easy way to visualize these curves is to note that if the peak of the radiation intensity was at the north-pole of the far-field hemisphere, then the meridional cut could be along the 0° and 180° meridian, whilst the cross cut would be along 90° and 270° meridian. Expressions for arbitrary great-circle curves, in stereographic coordinates, are given in the Supplementary Material (see Sec. VII).

Apart from cuts through the peak of radiation intensity it may be necessary to calculate the power radiated into a certain solid angle. Such calculations need to take into account the Jacobian of the stereographic coordinates $J = (2r/(1+u^2+v^2))^2$ (see Supplementary Materials; Sec. VI). Thus, given radiant intensity, i.e. power per solid angle, $I_\Omega(u, v) \propto r^2 |\mathbf{E}(u, v, r)|^2$, where \mathbf{E} is the electric field. The power (P_Ξ) radiated into a specific solid angle Ξ , i.e. a region in Fig. 2a, can be calculated as:

$$P_\Xi = \int_\Xi du dv I_\Omega(u, v) \left(\frac{2}{1+u^2+v^2} \right)^2$$

V. CONCLUSION

In summary, we have developed key properties of the stereographic coordinate system, which is induced by the (inverse) stereographic projection. Apart from providing a convenient, singularity-free, way of describing scalar fields on a surface of a hemisphere, such as radiation pattern from an illuminated aperture, for example, the stereographic coordinates give rise to singularity-free coordinate basis. Here we have shown that the stereographic coordinate basis is the Ludwig basis, already well-known in the field of antenna design. Knowledge of the coordinate system that gives rise to Ludwig basis, allows one, for example, to develop vector calculus tailored to Ludwig basis. Looking ahead, we expect that stereographic coordinates will find wide-spread use in the field of applied electromagnetism, particularly in areas where computers need to be taught to analyze radiation patterns from antennas, such as AI-aided antenna synthesis.

REFERENCES

- [1] C. A. Balanis. *Antenna theory*. John Wiley & Sons, 3rd edition, 2005.
- [2] C. E. Collin. *Antennas and Radiowave Propagation*. McGraw-Hill, 1985.
- [3] P. Moon and D. E. Spencer. *Field theory handbook*. Springer-Verlag, 2nd edition, 1971.
- [4] G. B. Arfken, H. J. Weber, and F. E. Harris. *Mathematical methods for physicists*. Academic Press, 7th edition, 2013.
- [5] H. Flanders. *Differential Forms*. Dover Publications, 1989.

- [6] A. C. Ludwig. The definition of cross polarization. *IEEE Tran. Antennas Propag.*, AP-21:116–119, 1973.
- [7] R. J. Howarth. History of the stereographic projection and its early use in geology. *Terra Review*, page 499, 1996.
- [8] B. A. Rosenfeld and N. D. Sergeeva. *Stereographic Projection*. MIR Publishers, Moscow, 1977.
- [9] R. J. Lisle and P.R. Leyshon. *Stereographic projection techniques for geologists and civil engineers*. Cambridge University Press, 2nd edition, 2014.
- [10] S. V. Haziot, and K. Marynets. Applying the stereographic projection to modeling of the flow of the antarctic circumpolar current. *Oceanography*, 31(3):68–75, 2018. <https://doi.org/10.5670/oceanog.2018.311>.
- [11] C. Xiao and M. G. Rossmann. Interpretation of electron density with stereographic roadmap prjections. *Journal of Structural Biology*, 158:182–187, 2007.
- [12] H. Liu and J. Liu. Sp2: a computer program for plotting stereographic projection and exploring crystallographic orientation relationships. *Journal of Applied Crystallography*, 45:130–134, 2011.
- [13] D. Roşca and J.-P. Antoine. Locally supported orthogonal wavelet bases on the sphere via stereographic projection. *Mathematical Problems in Engineering*, 2009:124904, 2009. doi:10.1155/2009/124904.
- [14] B. Schutz. *Geometrical methods of mathematical physics*. Cambridge University Press, 1999.
- [15] D. Lovelock and H. Rund. *Tensors, differential forms, and variational principles*. Dover Publications, 1989.
- [16] D. Bachman. *A geometric approach to differential forms*. Birkhäuser, 2nd edition, 2006.
- [17] J. M. Lee. *Introduction to smooth manifolds*. Springer, New York Heidelberg Dordrecht London, 2013.
- [18] T. Frankel. *The geometry of physics*. Cambridge University Press, 3rd edition, 2012.

VI. APPENDIX: VECTOR CALCULUS

The aim of this section is to calculate the common vector-calculus expressions in stereographic coordinates. To accomplish this task we will be relying on exterior derivative $d \dots$, Hodge star \star , as well as normal \mathbf{g} and and inverse \mathbf{g}^{-1} metric tensors [14]. Starting with the latter two, metric tensor is a bi-linear map that maps two vectors onto a real-valued scalar (at every point of the considered manifold). Representing the metric tensor as a matrix, for the case of stereographic coordinates:

$$\begin{aligned} \mathbf{g} &= \begin{pmatrix} g_{uu} & 0 & 0 \\ 0 & g_{vv} & 0 \\ 0 & 0 & g_{rr} \end{pmatrix} \\ &= \begin{pmatrix} \mathbf{e}_u \cdot \mathbf{e}_u & 0 & 0 \\ 0 & \mathbf{e}_v \cdot \mathbf{e}_v & 0 \\ 0 & 0 & \hat{\mathbf{r}} \cdot \hat{\mathbf{r}} \end{pmatrix} \\ &= \begin{pmatrix} \frac{4r^2}{\alpha^2} & 0 & 0 \\ 0 & \frac{4r^2}{\alpha^2} & 0 \\ 0 & 0 & 1 \end{pmatrix} \end{aligned}$$

Where $\alpha = 1 + u^2 + v^2$. The expression above can be used to extract the Jacobian for the stereographic coordinates [15]:

$$J = \sqrt{\det[\mathbf{g}]} = \frac{4r^2}{\alpha^2}$$

We denote the map from a single vector to a real-valued scalar, based on some vector \mathbf{q} , as $\mathbf{g}(\mathbf{q}, \bullet)$. Then for any vector \mathbf{p} :

$$(\mathbf{g}(\mathbf{q}, \bullet))(\mathbf{p}) = \mathbf{g}(\mathbf{q}, \mathbf{p}) = \text{scalar}$$

Since $\mathbf{g}(\mathbf{q}, \bullet)$ maps vectors to scalars (and is linear), it is a 1-form [16]. The metric tensor maps vectors to 1-forms (this is also known as musical isomorphisms [17]). Using non-normalized basis for vectors (and bearing in mind that $\mathbf{e}_r = \frac{d}{dr} = \hat{\mathbf{r}}$, i.e. radial basis vector is normalized from the outset):

$$\begin{aligned} \mathbf{g}(\mathbf{e}_u, \bullet) &= \frac{4r^2}{\alpha^2} du \\ \mathbf{g}(\mathbf{e}_v, \bullet) &= \frac{4r^2}{\alpha^2} dv \\ \mathbf{g}(\hat{\mathbf{r}}, \bullet) &= dr \end{aligned}$$

The inverse metric tensor maps pairs of 1-forms to real-

valued scalars:

$$\begin{aligned}
\mathbf{g}^{-1} &= \begin{pmatrix} g^{uu} & 0 & 0 \\ 0 & g^{vv} & 0 \\ 0 & 0 & g^{rr} \end{pmatrix} \\
&= \begin{pmatrix} \mathbf{d}u \cdot \mathbf{d}u & 0 & 0 \\ 0 & \mathbf{d}v \cdot \mathbf{d}v & 0 \\ 0 & 0 & \mathbf{d}r \cdot \mathbf{d}r \end{pmatrix} \\
&= \begin{pmatrix} 1/g_{uu} & 0 & 0 \\ 0 & 1/g_{vv} & 0 \\ 0 & 0 & 1/g_{rr} \end{pmatrix} \\
&= \begin{pmatrix} \frac{\alpha^2}{4r^2} & 0 & 0 \\ 0 & \frac{\alpha^2}{4r^2} & 0 \\ 0 & 0 & 1 \end{pmatrix}
\end{aligned}$$

Equivalently:

$$\begin{aligned}
\mathbf{g}^{-1}(\mathbf{d}u, \bullet) &= \frac{\alpha^2}{4r^2} \mathbf{e}_u \\
\mathbf{g}^{-1}(\mathbf{d}v, \bullet) &= \frac{\alpha^2}{4r^2} \mathbf{e}_v \\
\mathbf{g}^{-1}(\mathbf{d}r, \bullet) &= \hat{\mathbf{r}}
\end{aligned}$$

The volume form in stereographic coordinates is $\omega = \sqrt{g} \mathbf{d}u \wedge \mathbf{d}v \wedge \mathbf{d}r = \frac{4r^2}{\alpha^2} \mathbf{d}u \wedge \mathbf{d}v \wedge \mathbf{d}r$ [15], [18]. Based on it the action of Hodge star on individual forms is:

$$\begin{aligned}
\star 1 &= \frac{4r^2}{\alpha^2} \mathbf{d}u \wedge \mathbf{d}v \wedge \mathbf{d}r \\
\star \mathbf{d}u &= \mathbf{d}v \wedge \mathbf{d}r \\
\star \mathbf{d}v &= \mathbf{d}r \wedge \mathbf{d}u \\
\star \mathbf{d}r &= \frac{4r^2}{\alpha^2} \mathbf{d}u \wedge \mathbf{d}v \\
\star(\mathbf{d}u \wedge \mathbf{d}v) &= \frac{\alpha^2}{4r^2} \mathbf{d}r \\
\star(\mathbf{d}v \wedge \mathbf{d}r) &= \mathbf{d}u \\
\star(\mathbf{d}r \wedge \mathbf{d}u) &= \mathbf{d}v \\
\star(\mathbf{d}u \wedge \mathbf{d}v \wedge \mathbf{d}r) &= \frac{\alpha^2}{4r^2}
\end{aligned}$$

Using the equations above one can readily tackle a large portion of the standard tasks in vector calculus, as will be shown in the following sub-sections.

A. Gradient

The equation for vector-field ∇f , i.e. a gradient of some function, is [5], [18]:

$$\begin{aligned}
\nabla f &= g^{-1}(\mathbf{d}f, \bullet) \\
&= g^{-1}(\partial_u f \mathbf{d}u + \partial_v f \mathbf{d}v + \partial_r f \mathbf{d}r, \bullet) \\
&= \frac{\alpha^2}{4r^2} \partial_u f \mathbf{e}_u + \frac{\alpha^2}{4r^2} \partial_v f \mathbf{e}_v + \partial_r f \hat{\mathbf{r}}
\end{aligned}$$

Using Eq. (14, 15), i.e. $\mathbf{e}_u = \hat{\mathbf{i}}_{cross} \cdot 2r/\alpha$ and $\mathbf{e}_v = \hat{\mathbf{i}}_{ref} \cdot 2r/\alpha$:

$$\begin{aligned}
\nabla f &= \frac{\alpha}{2r} \partial_u f \hat{\mathbf{u}} + \frac{\alpha}{2r} \partial_v f \hat{\mathbf{v}} + \partial_r f \hat{\mathbf{r}} \\
&= \frac{\alpha}{2r} \partial_u f \hat{\mathbf{i}}_{cross} + \frac{\alpha}{2r} \partial_v f \hat{\mathbf{i}}_{ref} + \partial_r f \hat{\mathbf{r}}
\end{aligned}$$

B. Divergence

Given vector field $\mathbf{A} = A^u \mathbf{e}_u + A^v \mathbf{e}_v + A^r \mathbf{e}_r$, where $\mathbf{e}_r = \hat{\mathbf{r}}$, the equation for its divergence becomes [5], [18]:

$$\begin{aligned}
\nabla \cdot \mathbf{A} &= \star \mathbf{d} \star \mathbf{g}(\mathbf{A}, \bullet) \\
&= \star \mathbf{d} \star \left(\mathbf{d}u \frac{4r^2}{\alpha^2} A^u + \mathbf{d}v \frac{4r^2}{\alpha^2} A^v + \mathbf{d}r A^r \right) \\
&= \star \mathbf{d} \left(\frac{4r^2}{\alpha^2} A^u \mathbf{d}v \wedge \mathbf{d}r \right) + \star \mathbf{d} \left(\frac{4r^2}{\alpha^2} A^v \mathbf{d}u \wedge \mathbf{d}r \right) + \\
&\quad + \star \mathbf{d} \left(\frac{4r^2}{\alpha^2} A^r \mathbf{d}u \wedge \mathbf{d}v \right) \\
&= \star \left\{ \left(\partial_u \left(\frac{4r^2}{\alpha^2} A^u \right) + \partial_v \left(\frac{4r^2}{\alpha^2} A^v \right) + \right. \right. \\
&\quad \left. \left. + \partial_r \left(\frac{4r^2}{\alpha^2} A^r \right) \right) \mathbf{d}u \wedge \mathbf{d}v \wedge \mathbf{d}r \right\} \\
&= \frac{\alpha^2}{4r^2} \left\{ \left(\partial_u \left(\frac{4r^2}{\alpha^2} A^u \right) + \partial_v \left(\frac{4r^2}{\alpha^2} A^v \right) + \right. \right. \\
&\quad \left. \left. + \partial_r \left(\frac{4r^2}{\alpha^2} A^r \right) \right) \right\} \\
&= \alpha^2 \partial_u \left(\frac{A^u}{\alpha^2} \right) + \alpha^2 \partial_v \left(\frac{A^v}{\alpha^2} \right) + \frac{1}{r^2} \partial_r (r^2 A^r)
\end{aligned}$$

Using Eq. (14, 15), i.e. $\mathbf{e}_u = \hat{\mathbf{i}}_{cross} \cdot 2r/\alpha$ and $\mathbf{e}_v = \hat{\mathbf{i}}_{ref} \cdot 2r/\alpha$:

$$\begin{aligned}
\mathbf{A} &= A^u \mathbf{e}_u + A^v \mathbf{e}_v + A^r \hat{\mathbf{r}} \\
&= \frac{2r}{\alpha} A^u \hat{\mathbf{i}}_{cross} + \frac{2r}{\alpha} A^v \hat{\mathbf{i}}_{ref} + A^r \hat{\mathbf{r}}
\end{aligned}$$

Thus:

$$\begin{aligned}
A^u &= \frac{\alpha}{2r} \hat{\mathbf{i}}_{cross} \cdot \mathbf{A} = \frac{\alpha}{2r} \hat{\mathbf{u}} \cdot \mathbf{A} \\
A^v &= \frac{\alpha}{2r} \hat{\mathbf{i}}_{ref} \cdot \mathbf{A} = \frac{\alpha}{2r} \hat{\mathbf{v}} \cdot \mathbf{A} \\
A^r &= \hat{\mathbf{r}} \cdot \mathbf{A}
\end{aligned}$$

Therefore:

$$\begin{aligned}
\nabla \cdot \mathbf{A} &= \alpha^2 \partial_u \left(\frac{\hat{\mathbf{u}} \cdot \mathbf{A}}{2r\alpha} \right) + \alpha^2 \partial_v \left(\frac{\hat{\mathbf{v}} \cdot \mathbf{A}}{2r\alpha} \right) + \\
&\quad + \frac{1}{r^2} \partial_r (r^2 \hat{\mathbf{r}} \cdot \mathbf{A})
\end{aligned}$$

C. Curl

Curl of a vector field $\mathbf{A} = A^u \mathbf{e}_u + A^v \mathbf{e}_v + A^r \mathbf{e}_r$, where $\mathbf{e}_r = \hat{\mathbf{r}}$, can be expressed as [5], [18]:

$$\nabla \times \mathbf{A} = \mathbf{g}^{-1}(\star \mathbf{d} \mathbf{g}(\mathbf{A}, \bullet), \bullet)$$

Ignoring the last step for now:

$$\begin{aligned}
\star \mathbf{dg}(\mathbf{A}, \bullet) &= \star \mathbf{d} \left(\mathbf{d}u \frac{4r^2}{\alpha^2} A^u + \mathbf{d}v \frac{4r^2}{\alpha^2} A^v + \mathbf{d}r A^r \right) \\
&= \star \left(-\mathbf{d}u \wedge \mathbf{d}v \partial_v \left(\frac{4r^2}{\alpha^2} A^u \right) + \right. \\
&\quad + \mathbf{d}r \wedge \mathbf{d}u \partial_r \left(\frac{4r^2}{\alpha^2} A^u \right) + \\
&\quad + \mathbf{d}u \wedge \mathbf{d}v \partial_u \left(\frac{4r^2}{\alpha^2} A^v \right) - \\
&\quad - \mathbf{d}v \wedge \mathbf{d}r \partial_r \left(\frac{4r^2}{\alpha^2} A^v \right) - \\
&\quad - \mathbf{d}r \wedge \mathbf{d}u \partial_u (A^r) + \\
&\quad \left. + \mathbf{d}v \wedge \mathbf{d}r \partial_v (A^r) \right) \\
&= \left(\partial_v (A^r) - \partial_r \left(\frac{4r^2}{\alpha^2} A^v \right) \right) \cdot \mathbf{d}u + \\
&\quad + \left(\partial_r \left(\frac{4r^2}{\alpha^2} A^u \right) - \partial_u (A^r) \right) \cdot \mathbf{d}v + \\
&\quad + \left(\partial_u \left(\frac{4r^2}{\alpha^2} A^v \right) - \right. \\
&\quad \left. - \partial_v \left(\frac{4r^2}{\alpha^2} A^u \right) \right) \cdot \frac{\alpha^2}{4r^2} \cdot \mathbf{d}r
\end{aligned}$$

Applying the last step to change 1-forms to vectors:

$$\begin{aligned}
\mathbf{g}^{-1}(\star \mathbf{dg}(\mathbf{A}, \bullet), \bullet) &= \\
&= \left(\partial_v (A^r) - \partial_r \left(\frac{4r^2}{\alpha^2} A^v \right) \right) \cdot \frac{\alpha^2}{4r^2} \mathbf{e}_u + \\
&\quad + \left(\partial_r \left(\frac{4r^2}{\alpha^2} A^u \right) - \partial_u (A^r) \right) \cdot \frac{\alpha^2}{4r^2} \mathbf{e}_v + \\
&\quad + \left(\partial_u \left(\frac{4r^2}{\alpha^2} A^v \right) - \partial_v \left(\frac{4r^2}{\alpha^2} A^u \right) \right) \cdot \frac{\alpha^2}{4r^2} \cdot \hat{\mathbf{r}}
\end{aligned}$$

Finally, expressing all in normalized basis:

$$\begin{aligned}
\nabla \times \mathbf{A} &= \frac{\alpha}{2r} \cdot \left(\partial_v (\hat{\mathbf{r}} \cdot \mathbf{A}) - \partial_r \left(\frac{2r}{\alpha} \hat{\mathbf{v}} \cdot \mathbf{A} \right) \right) \cdot \hat{\mathbf{u}} + \\
&\quad + \frac{\alpha}{2r} \cdot \left(\partial_r \left(\frac{2r}{\alpha} \hat{\mathbf{u}} \cdot \mathbf{A} \right) - \partial_u (\hat{\mathbf{r}} \cdot \mathbf{A}) \right) \cdot \hat{\mathbf{v}} + \\
&\quad + \frac{\alpha^2}{4r^2} \cdot \left(\partial_u \left(\frac{2r}{\alpha} \hat{\mathbf{v}} \cdot \mathbf{A} \right) - \partial_v \left(\frac{2r}{\alpha} \hat{\mathbf{u}} \cdot \mathbf{A} \right) \right) \cdot \hat{\mathbf{r}}
\end{aligned}$$

VII. APPENDIX: GREAT CIRCLES ON THE HEMI-SPHERE

The aim of this section is to derive equation for an arbitrary great circle, i.e. a curve on the surface of a sphere created by intersection of the sphere surface with a plane that passes through the centre of the sphere. Great circles are geodesic curves on spheres [14]. For purposes of this section it is easier to derive main results in Cartesian coordinates xyz and then to connect them to stereographic coordinates using Eq. (7, 8, 9).

The great circle will be obtained by starting from a great circle in the xz -plane that goes around the y -axis in counter-clockwise direction:

$$\mathcal{C}'''(\psi) = \begin{pmatrix} r \sin \psi \\ 0 \\ r \cos \psi \end{pmatrix}$$

The aim is to rotate this great circle to go through point $P_0 = (\theta_0, \phi_0) = (60^\circ, 30^\circ)$, in spherical coordinates, at $\psi = 0$. Simultaneously it is desirable to have an additional parameter to control in which direction the great circle points as ψ grows, call this parameter Φ . Begin by rotating the curve \mathcal{C}''' around the z by Φ to get \mathcal{C}'' :

$$\begin{aligned}
\mathcal{C}''(\psi) &= \begin{pmatrix} \cos \Phi & -\sin \Phi & 0 \\ \sin \Phi & \cos \Phi & 0 \\ 0 & 0 & 1 \end{pmatrix} \mathcal{C}'''(\psi) \\
&= \begin{pmatrix} r \cos \Phi \sin \psi \\ r \sin \Phi \sin \psi \\ r \cos \psi \end{pmatrix}
\end{aligned}$$

The result, \mathcal{C}'' , still goes through north pole, but the tangent to \mathcal{C}'' , at the north pole, is now at angle Φ relative to the y -axis. Next rotate \mathcal{C}'' around y -axis by angle θ_0 to get \mathcal{C}' :

$$\begin{aligned}
\mathcal{C}'(\psi) &= \begin{pmatrix} \cos \theta_0 & 0 & \sin \theta_0 \\ 0 & 1 & 0 \\ -\sin \theta_0 & 0 & \cos \theta_0 \end{pmatrix} \mathcal{C}''(\psi) \\
&= \begin{pmatrix} r \cos \Phi \cos \theta_0 \sin \psi + r \sin \theta_0 \cos \psi \\ r \sin \Phi \sin \psi \\ -r \cos \Phi \sin \theta_0 \sin \psi + r \cos \theta_0 \cos \psi \end{pmatrix}
\end{aligned}$$

This will bring the point of $\psi = 0$ to the correct latitude (θ_0) of the destination. Finally, rotate around z -axis by ϕ_0 to get curve \mathcal{C} which has point $\psi = 0$ at P_0 :

$$\mathcal{C}(\psi) = \begin{pmatrix} \cos(\phi_0) & -\sin(\phi_0) & 0 \\ \sin(\phi_0) & \cos(\phi_0) & 0 \\ 0 & 0 & 1 \end{pmatrix} \mathcal{C}'(\psi)$$

The result is a great circle that goes through P_0 , as needed, and can be pointed in any direction by adjusting Φ . Figure VIIa shows two great circles going through P_0 in such a way that their tangents are perpendicular at that point.

Using Eq. (7, 8) the expressions for the great circles on a hemi-sphere in stereographic coordinates become:

$$\begin{aligned}
u(\psi; \Phi, \theta_0, \phi_0) &= \left(\cos \Phi \cos \theta_0 \cos \phi_0 \sin \psi - \right. \\
&\quad \left. - \sin \Phi \sin \phi_0 \sin \psi + \sin \theta_0 \cos \phi_0 \cos \psi \right) \times \\
&\quad \times \left(1 - \cos \Phi \sin \theta_0 \sin \psi + \cos \theta_0 \cos \psi \right)^{-1} \quad (16)
\end{aligned}$$

$$\begin{aligned}
v(\psi; \Phi, \theta_0, \phi_0) = & \left(\cos \Phi \cos \theta_0 \sin \phi_0 \sin \psi + \right. \\
& \left. + \sin \Phi \cos \phi_0 \sin \psi + \sin \theta_0 \sin \phi_0 \cos \psi \right) \times \\
& \times \left(1 - \cos \Phi \sin \theta_0 \sin \psi + \cos \theta_0 \cos \psi \right)^{-1} \quad (17)
\end{aligned}$$

Figure VIIb shows the great-circle curves, in the north hemi-sphere, plotted in stereographic projection, with u and v as Cartesian coordinates.

VIII. RADIATION FROM SQUARE APERTURE ILLUMINATED WITH PHASE GRADIENT

Here we restate the result from [2] (Sec. 4.1) specific to the situation at hand. For a square aperture, lying in the xy -plane, with centre at origin, and driven with electric field $\mathbf{E} = E_0 \hat{\mathbf{x}} \exp(-i(\zeta_x x + \zeta_y y))$, the far-field radiation is given by (see Eq. (4.24) in ref. [2]):

$$\begin{aligned}
\mathbf{E}(r, \theta, \phi) = & \frac{ik_0 4a^2 E_0}{2\pi r} \cdot \exp(-ik_0 r) \times \\
& \times \frac{\sin(a \cdot [k_0 \sin \theta \cos \phi - \zeta_x])}{a \cdot [k_0 \sin \theta \cos \phi - \zeta_x]} \times \frac{\sin(a \cdot [k_0 \sin \theta \sin \phi - \zeta_y])}{a \cdot [k_0 \sin \theta \sin \phi - \zeta_y]} \\
& \times \left(\hat{\boldsymbol{\theta}} \cos \phi - \hat{\boldsymbol{\phi}} \sin \phi \cos \theta \right)
\end{aligned}$$

Restating the problem in stereographic coordinates (using Eq. (3, 4, 12, 13)):

$$\begin{aligned}
\mathbf{E}(u, v, r) = & \frac{ik_0 4a^2 E_0}{2\pi r} \times \exp(-ik_0 r) \times \\
& \times \frac{\sin(a \cdot [2k_0 u/\alpha - \zeta_x])}{a \cdot [2k_0 u/\alpha - \zeta_x]} \times \frac{\sin(a \cdot [2k_0 v/\alpha - \zeta_y])}{a \cdot [2k_0 v/\alpha - \zeta_y]} \times \\
& \times \left(\left[\frac{u^2(1+u^2) + v^2(1-v^2)}{(u^2+v^2)\alpha} \right] \hat{\mathbf{u}} + \left[\frac{2uv}{\alpha} \right] \hat{\mathbf{v}} \right)
\end{aligned}$$

Where $\alpha = 1 + u^2 + v^2$.

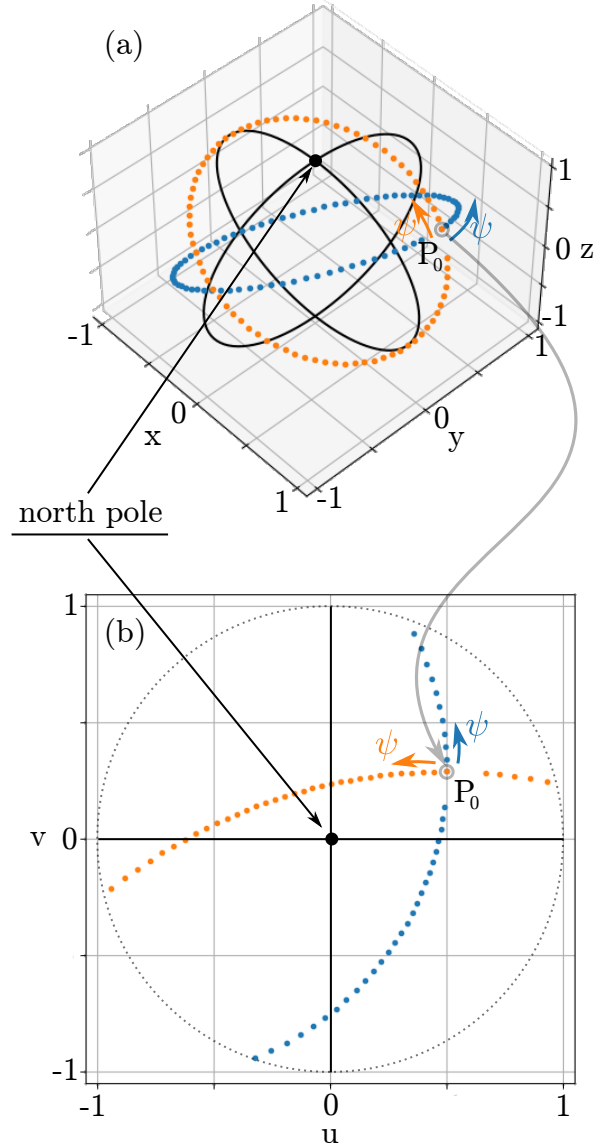


Figure 3. **Two great circles intersecting at a common point P_0 .** (a) The actual shape of the two great circles in the 3d space. The great circles, orange and blue, are plotted as sets of disconnected dots distributed uniformly (fixed steps in ψ) along the great circle. Parameter ψ is the arc-length along the great circles divided by the radius of the sphere. Point P_0 corresponds to $\psi = 0$ on both great circles. The orange and blue arrows point in the direction of growing ψ . The last section of the blue and orange great circles, i.e. where ψ is at maximum value (see Eq. (16, 17)), is omitted to show where each great circle starts and ends. The black circles are meridians used to outline the underlying sphere. Meridian intersection at the north pole is marked with a bold dot. (b) The u and v stereographic coordinates for the points of the two great circles in the north hemi-sphere. The changing distance between the dots in the projected great circles shows the distortion that arises as a result of stereographic projection.